Using 18-Fluoro-2-Deoxyglucose Positron Emission Tomography in Detecting Infectious Endocarditis/ Endoarteritis:

A Preliminary Report[1]

Ruoh-Fang Yen, MD, Yee-Chun Chen, MD, PhD, Yen-Wen Wu, MD, Mei-Hsiu Pan, MD, Shan-Chwen Chang, MD, PhD

Rationale and Objectives. We evaluated the effectiveness of positron emission tomography (PET) with 18-fluoro-2-deoxyglucose (FDG) in the detection of infectious endocarditis/endoarteritis.

Materials and Methods. For this study, we recruited 6 patients (4 women, 2 men; age range, 35 – 78 years; mean age, 55.8 ± 16.8 years) who were clinically diagnosed as having infective endocarditis/endoarteritis by their echocardiographic findings and by Duke criteria.

Results. For all 6 patients, we also found increased FDG uptakes in the corresponding areas detected in echocardiography.

Conclusion. FDG-PET appears to be a promising tool in diagnosing infective endocarditis/endoarteritis, and further prospective studies on a large scale to fully exploit the usefulness of FDG-PET for infective endocarditis/endoarteritis are needed.

Key Words. 18-Fluoro-2-deoxyglucose; positron emission tomography; infective endocarditis; infective endoarteritis.

Echocardiography plays an important role in the diagnosis of infective endocarditis/endoarteritis (1–5). It allows the detection of vegetations and estimation of valvular dysfunction (2–7). However, vegetations identified in echocardiography may not correspond to active inflammatory processes. In certain circumstances, for patients with prosthetic valves and for patients who had previous cardiac surgery, vegetations may not be identified by echocardiography (4,6). Nuclear medicine procedures, such as gallium-67 scintigraphy, indium-111 leukocyte scintigraphy, technecium-99m- HMPAO leukocyte scintigraphy, etc., are occasionally called in as supplementary diagnosing tools for infective endocarditis/endoarteritis (8–20). Nevertheless, these imaging modalities have not been widely adopted due to the limitation of the spatial resolutions of these scintigraphies that are unable to resolve small vegetations.

18-Fluoro-2-deoxyglucose positron emission tomography (FDG-PET) is effective in the early detection of many malignancies. Inflammatory processes also result in significant FDG uptake (21–25). Infective endocarditis/ endoarteritis is usually characterized by vegetations, which are composed of platelets, fibrins, microorganisms, and inflammatory cells. Increased FDG uptakes may thus also appear in the vegetations. This pilot study is designed to evaluate the effectiveness of FDG-PET in the detection of infectious endocarditis/endoarteritis.

Acad Radiol 2004; 11:316–321

[1] From the Departments of Nuclear Medicine (R.F.Y., Y.W.W., M.H.P.) and Internal Medicine (Y.C.C., S.C.C.), National Taiwan University Hospital and National Taiwan University College of Medicine, No. 7, Chung-Shan South Road, Taipei 10016, Taiwan. Received September 28, 2003; revision requested October 20; received in revised form November 4; accepted November 6. **Address correspondence to** R.-F.Y. E-mail: rfyen@ha.mc.ntu.edu.tw

doi:10.1016/S1076-6332(03)00715-3

Table 1
Patients' characteristics, echocardiographic and FDG-PET results

Patient	Age in years, sex	Underlying condition	Microorganism from blood culture	Echocardiography	FDG-PET	Lesion-to-lung ratio	Myocardium-to-lung ratio
1	51,M	Dilated aortic root after Bentall's procedure	Salmonellar	Soft tissue density at aortic root	FDG hypermetabolism at aortic root	8.4	No myocardial uptake
2	62,F	RHD with MR, MS, AR, anemia	N/I	Thrombus in LA appendage	Increased FDG metabolism in LA appendage	3.3	No myocardial uptake
3	69,F	RHD with MS	*E. coli*	Thrombus in LA	Increased FDG metabolism in LA and aorta	3.0	No myocardial uptake
4	35,F	Anemia, severe TR, dilated RV	*Staphylococcus aureus*	Small vegetation on TV	FDG hypermetabolic spot at TV region	3.0	6.5
5	40,M	Marfan's disease with Type 1 aortic dissection after Bentall's procedure	Staphylococci	Soft tissue around mechanical AV	Increased FDG metabolism at AV region	3.1	15.8
6	78,F	Old ischemic stroke with left hemiparesis	*Staphylococcus epidermidis*	AV vegetation	Increased FDG metabolism at AV region	3.1	10.8

Abbreviations: AR, aortic regurgitation; AV, aortic valve; LA, left atrium; MR, mitral regurgitation; MS, mitral stenosis; N/I, none identified; RHD, rheumatic heart disease; RV, right ventricle; TR, tricuspid regurgitation; TV, tricuspid valve.

MATERIALS AND METHODS

Patients

From May 2001 to January 2003, 6 patients (4 women, 2 men; age range, 35–78 years; mean age, 55.8 $\pm$ 16.8 years), who were clinically diagnosed as having infective endocarditis/endoarteritis by echocardiographic findings and by Duke criteria (1) were recruited for this study. None of them had diabetes mellitus. The basic characteristics and clinical details of these patients are listed in Table 1.

FDG-PET

FDG-PET was performed within 1 week of echocardiography. Before the FDG-PET study, each patient fasted for 6 hours or more. FDG-PET imaging was performed using a GE advance PET scanner (GE Medical Systems, Milwaukee, WI). The GE advance PET scanner produced 4.25-mm thick image planes (18 direct planes and 17 cross planes). The axial field of view was 15 cm and the full width of half maximum (FWHM) was 5 mm. Acquisitions for the emission data began 45 minutes after intravenous injection of 370 MBq (10 mCi) FDG. From the collected emission data that had been corrected for scatter, random events, and dead time, the image was reconstructed using ordered-subset expectation maximization without attenuation correction. Image pixel size was 3.0 mm in a 128 $\times$ 128 array. The transversal PET images were individually reoriented into coronal and sagittal planes to obtain a better view of the chest.

Image Interpretation

The FDG-PET images were interpreted by two experienced nuclear medicine physicians, who had knowledge of the prior echocardiographic findings. The lesion areas were identified by consensus of both physicians, and their lesion-to-lung FDG uptake ratios were then measured. The myocardium-to-lung ratios were also calculated if FDG uptakes in the left ventricular (LV) myocardium were noted.

RESULTS

For all 6 patients, we also found increased FDG uptakes in the corresponding areas of vegetations detected in

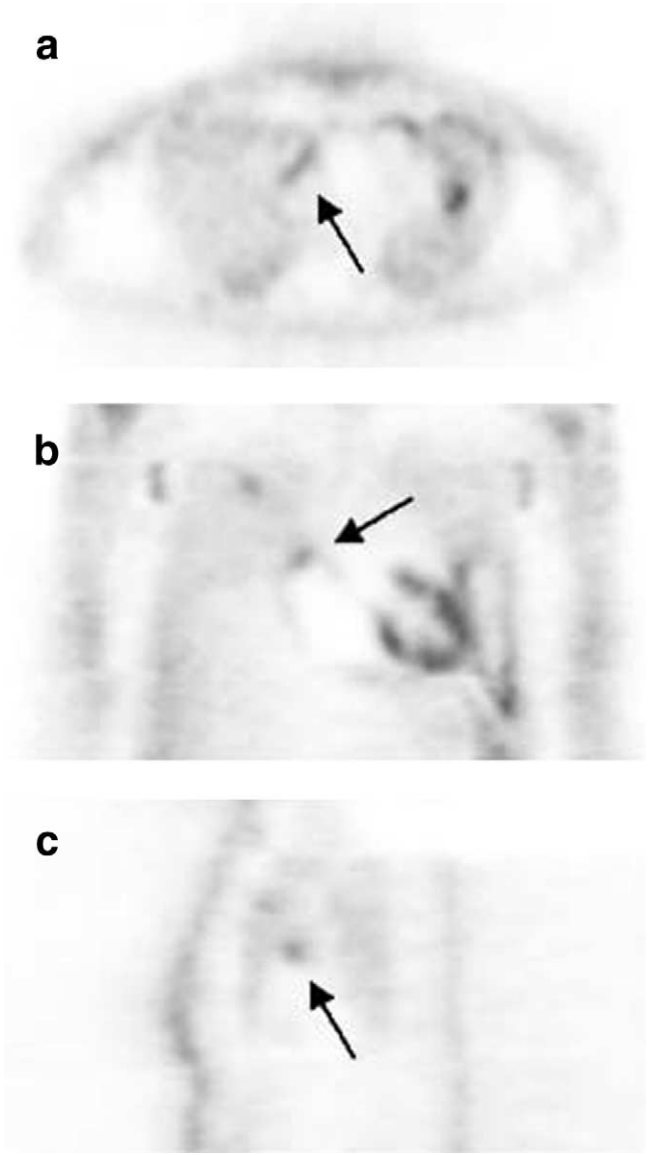

Figure 1. A 35-year-old female (case 4) presented with methicillin-sensitive staphylococcus aureus in her blood culture. The echocardiography revealed small vegetation at the tricuspid valve. The FDG-PET axial **(a)**, coronal **(b)** and sagittal **(c)** images demonstrated FDG uptake in the LV myocardium, the dilated right ventricle, and a focal area of hypermetabolism at the inlet of the right ventricle **(arrows)**.

echocardiography (Table 1). The abnormal FDG uptakes were easily detectable, and their lesion-to-lung values ranged from 3.0 to 8.4. FDG uptakes in the LV myocardium were noted in 3 of the 6 patients and the myocardium-to-lung ratios are listed in the last column of Table 1.

In Figure 1, we have included the FDG-PET images for patient 4 of Table 1. This patient was a 35-year-old female with methicillin-sensitive staphylococcus aureus in her blood culture. The echocardiography revealed small vegetation at the tricuspid valve. The FDG-PET images demonstrated FDG uptake in the LV myocardium. The images also showed a focal area of hypermetabolism at the inlet of the dilated right ventricle whose location was consistent with the findings from echocardiography.

The FDG-PET images patient 1 of Table 1 are also included in Figure 2. This 51-year-old male patient was admitted because of intermittent fever for 5 days. He was suffered from dilated aortic root and had gone through Bentall's procedure 9 years ago. The echocardiography, which was performed after the discovery of Salmonella in his blood culture, revealed soft tissue density at the aortic root. Subsequent FDG-PET images also showed hypermetabolism in the corresponding areas (arrows). No myocardial uptake was found for this patient.

Note that we have also included in Figure 3 the FDG-PET images of another 79-year-old female patient, who is not one of the 6 aforementioned patients. This patient was hospitalized because of exertional dyspnea. Her echocardiography revealed severe aortic stenosis without vegetation. She did not appear to have infective endocarditis or endoarteritis clinically. No abnormal FDG uptake on the stenotic aortic valves was visible in her FDG-PET images.

DISCUSSION

In addition to clinical and laboratory data, echocardiography based on the detection of vegetations is a primary tool in diagnosing infective endocarditis/endoarteritis (1–5). However, it has been noted that echocardiography is not faultless. Under certain circumstances, the vegetations detected by echocardiography may not be actively infective (4). Furthermore, small vegetations in patients with prosthetic valves may escape the detection of echocardiography due to the intense echoes generated by the prosthesis (5,6).

It is also known that anatomical imaging, such as chest radiography, computed tomography (CT), and magnetic resonance imaging, have only limited success in the diagnosis of infective endocarditis/endoarteritis (26–28). Scintigraphy of infection and inflammation using various radiopharmaceuticals has been occasionally used to supplement the diagnosis for infective endocarditis/endoarteritis (8–20). But the laborious and time-consuming procedure of cell labeling and the insufficient spatial resolution power of SPECT scintigraphy to handle small vegetations (2–4) with diameters less than 10 mm have hindered the

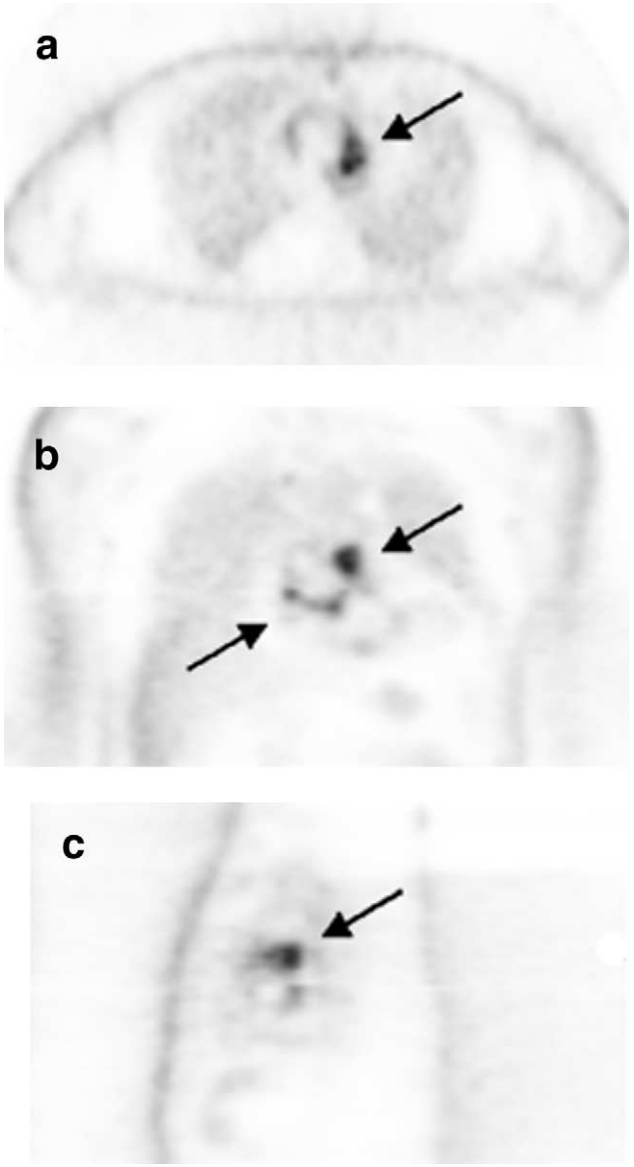

Figure 2. A 51-year-old male (case 1) was a suffered from dilated aortic root and had gone through Bentall's procedure 9 years ago. The echocardiography, which was performed after the discovery of Salmonella in his blood culture, revealed soft tissue density at the aortic root. Subsequent FDG-PET axial **(a)**, coronal **(b)**, and sagittal **(c)** images also showed hypermetabolism in the corresponding areas **(arrows)**. Myocardium uptake was absent.

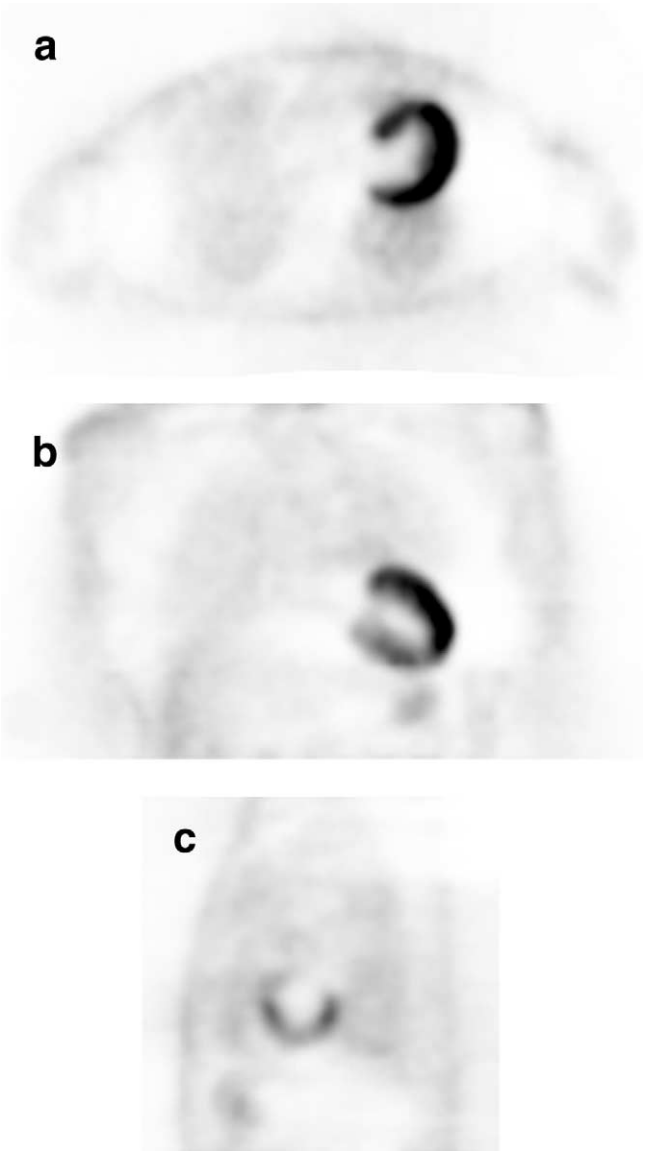

Figure 3. A 79-year-old female was hospitalized because of exertional dyspnea. Echocardiography revealed severe aortic stenosis without vegetation. She did not appear to have infective endocarditis or endoarteritis clinically. No abnormal FDG uptake on the stenotic aortic valves was visible in her FDG-PET axial **(a)**, coronal **(b)**, or sagittal **(c)** images. The images demonstrated FDG uptake in the LV myocardium with myocardium-to-lung ratio of 12.5.

popularity of these diagnoses. In our opinion, the clinical worthiness of these various scintigraphies remains to be proven.

It has been demonstrated that FDG uptakes accumulate rapidly in inflammatory and infectious lesions (21–24,29) with high and early target-to-background ratios (29). In addition, better spatial resolution of PET in comparison with SPECT makes the detection of small lesions possible. FDG-PET has already been clinically used to detect inflammatory and infectious lesions (30–32). In this study, we discover that FDG does accumulate in the infected vegetations.

Although all 6 patients in this study fasted for at least 6 hours before the FDG injections, FDG uptakes in the LV myocardium were noted in 3 of them. Nonetheless,

the uptakes of the LV myocardium didn't interfere with the interpretation. In fact, they became the landmarks for heart chambers and gave better localizations for the lesions. In addition to lesions of infected endocarditis/endoarteritis, it has been observed that FDG uptakes in mediastinum may also occur in other benign lesions, such as hyperplastic lymph nodes, tuberculosis lymphadenitis, sclerosing mediastinitis, sarcoidosis, benign cysts, hyperplasia of thymus, schwannoma, or teratoma (33–38). One should carefully correlate FDG-PET findings with patients' clinical history and other anatomical imaging findings to discern true positive from false positive results.

Recently, the combined PET/CT system offers significant advantages in the localization of focal uptake and in the differentiation of pathological uptake from the normal physiological uptake (39–41). However, it has been noted that when imaging with PET/CT, metallic implants and respiration-induced attenuation may induce artifacts and disturb the interpretation of PET images (42,43). It appears that further studies are required to clarify the extra benefits of applying combined PET/CT imaging over stand-alone PET for diagnosing infective endocarditis/endoarteritis.

We would like to point out that the FDG-PET images in this study were non-attenuation corrected. Although the signal-to-noise ratios might be improved with attenuation correction (44–46), the image resolutions without attenuation correction were already sufficient for our purpose.

No follow-up FDG-PET scan was taken for any of the 6 patients during their treatments and after their recoveries because of practical difficulties. In theory, successfully treated vegetations will not be visualized on the follow-up scan, but one has to be careful about the timing for performing the follow-up scan. It has been noted (32) that certain degrees of FDG uptakes may be observed for a patient during the healing phase after the completion of the antibiotic treatment.

In conclusion, the excellent agreements of FDG-PET and echocardiographic findings in this study, in spite of the scarcity of our sample cases, lead us to believe that FDG-PET is a promising supplementary diagnostic tool in addition to conventional echocardiography for identifying the foci of active infective endocarditis/endoarteritis. It is reasonable to expect that future prospective studies on a large scale will fully exploit the usefulness of FDG-PET for infective endocarditis/endoarteritis.

REFERENCES

1. Mylonakis E, Calderwood SB. Infective endocarditis in adults. N Engl J Med 2001; 345:1318–1330.
2. Dillon JC, Feigenbaum H, Konecke LL, et al. Echocardiographic manifestations of valvular vegetations. Am Heart J 1973; 86:698–704.
3. Yvorchuk KJ, Chan KL. Application of transthoracic and transesophageal echocardiography in the diagnosis and management of infective endocarditis. J Am Soc Echocardiog 1994; 7:294–308.
4. Mathew J, Anand A, Addai T, et al. Value of echocardiographic findings in predicting cardiovascular complications in infective endocarditis. Angiology 2001; 52:801–809.
5. Sachdev M, Peterson GE, Jollis JG. Imaging techniques for diagnosis of infective endocarditis. Infect Dis Clin N Am 2002; 16:319–337.
6. Cowgill LD, Addonizio VP, Hopeman AR, et al. A practical approach to prosthetic valve endocarditis. Ann Thorac Surg 1987; 43:450–457.
7. Kupferwasser LI, Darius H, Műller AM, et al. Diagnosis of culture-negative endocarditis: the role of the Duke criteria and the impact of transesophageal echocardiography. Am Heart J 2001; 142:146–152.
8. Ivančević V, Munz DL. Nuclear medicine imaging of endocarditis. Q J Nucl Med 1999; 43:93–99.
9. Gratz S, Raddatz D, Hagenah G, et al. ^{99m}Tc-labelled antigranulocyte monoclonal antibody FAB' fragments versus echocardiography in the diagnosis of subacute infective endocarditis. Int J Cardiol 2000; 75: 75–84.
10. Spies SM, Meyers SN, Barresi V, et al. A case of myocardial abscess evaluated by radionuclide techniques: case report. J Nucl Med 1977; 18:1089–1090.
11. Adams BK. Tc-99m leukocyte scintigraphy in infective endocarditis. Clin Nucl Med 1995; 20:395–397.
12. Morguet AJ, Munz DL, Ivančević V, et al. Immunoscintigraphy using technetium-99m-labeled anti-NCA-95 antigranulocyte antibodies as an adjunct to echocardiography in subacute infective endocarditis. J Am Coll Cardiol 1994; 23:1171–1178.
13. Cerqueira MD, Jacobson AF, Matsuda M, et al. Indium-111 leukocyte scintigraphic detection of mitral valve vegetations in active bacterial endocarditis. Am J Cardiol 1989; 64:1080–1081.
14. Cerqueira MD, Jacobson AF. Indium-111 leukocyte scintigraphic detection of myocardial abscess formation in patients with endocarditis. J Nucl Med 1989; 20:703–706.
15. Oates E, Sarno RC. Detection of a prosthetic aortic valvular abscess with indium-111-labeled leukocytes. Chest 1988; 94:872–874.
16. Miller SW, Palmer EL, Dinsmore RE, et al. Gallium-67 and magnetic resonance imaging in aortic root abscess. J Nucl Med 1987; 28:1616–1619.
17. Reinke FE, Yuille DL, Jackson LJ, et al. Cardiac aneurysm complicated by E. coli abscess. J Nucl Med 1983; 24:1154–1157.
18. Wiseman J, Rouleau J, Rigo P, et al. Gallium-67 myocardial imaging for the detection of bacterial endocarditis. Radiology 1976; 120:135–138.
19. Purnell GL, Walker CW, Allison JW, et al. Indium-111 leukocyte localization in infected prosthetic graft. Clin Nucl Med 1990; 15:585–586.
20. Pena FJ, Banzo I, Quirce R, et al. Ga-67 SPECT to detect endocarditis after replacement of an aortic valve. Clin Nucl Med 2002; 27:401–404.
21. Yamada S, Kubota K, Kubota R, et al. High accumulation of fluorine-18-fluorodeoxyglucose in turpentine-induced inflammatory tissue. J Nucl Med 1995; 36:1301–1306.
22. Kubota R, Yamada S, Kubota K, et al. Intratumoral distribution of fluorine-18-fluorodeoxyglucose in vivo: high accumulation in macrophages and granulation tissues studied by microautoradiography. J Nucl Med 1992; 33:1972–1980.
23. Tahara T, Ichiya Y, Kuwabara Y, et al. High [^{18}F]-fluorodeoxyglucose uptake in abdominal abscesses: a PET study. J Comput Assist Tomogr 1989; 13:829–831.
24. Sugawara Y, Gutowski TD, Fisher SJ, et alUptake of positron emission tomography tracers in experimental bacterial infectionsa comparative biodistribution study of radiolabeled FDG, thymidine, $_L$-methionine, ^{67}Ga-citrate, and ^{125}I-HSA. Eur J Nucl Med 1999; 26:333–341.

25. Yen RF, Chen ML, Liu FY, et alFalse-positive 2- [F-18]-fluoro-2-deoxy-D-glucose positron emission tomography studies for evaluation of focal pulmonary abnormalities. J Formos Med Assoc 1998; 97:642–645.
26. Cowan JC, Patrick D, Reid DS. Aortic root abscess complicating bacterial endocarditis demonstration by computed tomography. Br Heart J 1984; 52:591–593.
27. Jeang MK, Fuentes F, Gately A, et al. Aortic root abscess: initial experience using magnetic resonance imaging. Chest 1986; 89:613–615.
28. Winkler ML, Higgins CB. MRI of perivalvular infectious pseudoaneurysms. Am J Roentgenol 1986; 147:253–256.
29. Gutowski TD, Fisher SJ, Moon S, et alExperimental studies of 18F-2-fluoro-2-deoxy-D-glucose (FDG) in infection and in reactive lymph nodes [abstract]. J Nucl Med 1992; 33:925p.
30. Stumpe KDM, Dazzi H, Schaffner A, et al. Infection imaging using whole-body FDG-PET. Eur J Nucl Med 2000; 27:822–832.
31. Sugawara Y, Braun DK, Kison PV, et al. Rapid detection of human infections with fluorine-18 fluorodeoxyglucose and positron emission tomography: preliminary results. Eur J Nucl Med 1998; 25:1238–1243.
32. Klïcke T, Schmitz A, Risse JH, et al. Fluorine-18 fluorodeoxyglucose PET in infectious bone diseases: results of histologically confirmed cases. Eur J Nucl Med 2000; 27:524–528.
33. Boiselle PM, Patz EF Jr, Vining DJ, et al. Imaging of mediastinal lymph nodes: CT, MR, and FDG PET. Radiographics 1998; 18:1061–1069.
34. Kwan A, Seltzer M, Czernin J, et al. Characterization of hilar lymph node by 18F-fluoro-2-deoxyglucose positron emission tomography in healthy subjects. Anticancer Res 2001; 21:701–706.
35. Sun SS, Tsai SC, Hsieh JF, et al. False-positive uptake of ^{18}F-fluorodeoxyglucose in the hilar region and mediastinum. Semin Nucl Med 2001; 31:84–86.
36. Bakheet S, Powe J, Ezzat A, et al. F-18-FDG uptake in tuberculosis. Clin Nucl Med 1998; 23:739–742.
37. Imran MB, Kubota K, Yoshioka S, et al. Sclerosing mediastinitis: findings on fluorine-18 fluorodeoxyglucose positron emission tomography. Clin Nucl Med 1999; 24:305–308.
38. Kubota K, Yamada S, Kondo T, et al. PET imaging of primary mediastinal tumours. Br J Cancer 1996; 73:882–886.
39. Beyer T, Townsend DW, Brun T, et al. A combined PET/CT scanner for clinical oncology. J Nucl Med 2000; 41:1369–1379.
40. Costa DC, Visvikis D, Crosdale I, et al. Positron emission and computed X-ray tomography: a coming together. Nucl Med Commun 2003; 24:351–358.
41. Ell PJ, von Schulthess GK. PET/CT: a new road map. Eur J Nucl Med 2002; 29:719–720.
42. Goerres GW, Ziegler SI, Burger C, et al. Artifacts at PET and PET/CT caused by metallic hip prosthetic material. Radiology 2003; 226:577–584.
43. Goerres GW, Burger C, Kamel E, et al. Respiration-induced attenuation artifact at PET/CT: technical considerations. Radiology 2003; 226: 906–910.
44. Bengel FM, Ziegler SI, Avril N, et al. Whole-body positron emission tomography in clinical oncology: comparison between attenuation-corrected and uncorrected images. Eur J Nucl Med 1997; 24:1091–1098.
45. Coleman RE, Laymon CM, Turkington TG. FDG imaging of lung nodules: a phantom study comparing SPECT, camera-based PET and dedicated PET. Radiology 1999; 210:823–828.
46. Nuyts J, Stroobants S, Dupont P, et al. Reducing loss of image quality because of the attenuation artifact in uncorrected PET whole-body images. J Nucl Med 2002; 43:1054–1062.